RSC Advances

PAPER

View Article Online
View Journal | View Issue

Cite this: *RSC Adv.*, 2016, **6**, 47298

A highly efficient magnetic solid acid nanocatalyst for the synthesis of new bulky heterocyclic compounds

Masoud Nasr-Esfahani,* Zahra Rafiee, Morteza Montazerozohori and Hassan Kashi

Received 29th January 2016
Accepted 4th May 2016

DOI: 10.1039/c6ra02749k

www.rsc.org/advances

Fe_3O_4 nanoparticles were prepared and coated with 3-aminopropyltriethoxysilane (APTES). The formed amine-surfaced Fe_3O_4@APTES NPs were further chemically modified with maleic anhydride (MAH) to generate Fe_3O_4@APTES·MAH NPs. This catalyst was characterized by FT-IR, X-ray diffraction (XRD), scanning electron microscopy (SEM), transmission electron microscopy (TEM), thermogravimetric analysis (TG), energy dispersive X-ray analyzer (EDAX), vibrating sample magnetometry (VSM) and the dynamic light scattering (DLS) measurement technique. The catalyst showed high thermal stability and good reusability. Some new bulky heterocyclic compounds such as bis(2,4,5-triarylimidazole), bis(1,4-dihydropyridine), bis(1,8-dioxooctahydroxanthene) and bis(1,8-dioxo-decahydroacridine) derivatives were synthesized using 4,4′-(alkylazanediyl)dibenzaldehyde as substrate and Fe_3O_4@APTES or Fe_3O_4@APTES·MAH as catalyst. The high purity products were isolated and the catalyst was easily separated with a simple work-up with magnetic field and was recycled several times without noticeable loss of reactivity under the described reaction conditions.

Introduction

Magnetic iron oxide (Fe_3O_4) nanoparticles have been widely used as a heterogeneous catalyst for the synthesis of heterocyclic compounds such as α-aminophosphonates,[1] 2,3-dihydroquinazolin-4(1*H*)-ones,[2] dihydropyrimidinone,[3] pyrans,[4] 1,4-dihydropyridines,[5] calix(4)resorcinarenes,[6] xanthenes,[7] acridines,[8] imidazoles,[9] Aza-Sakurai reaction[10] and Strecker reaction.[11] This compound has been investigated for various applications in biomedical sciences including detoxification of biological fluids, anti-cancer drug delivery, food analysis, environmental treatment and magnetic resonance imaging (MRI).[12–19]

The magnetic iron oxide NPs have intrinsic instability over longer periods, because they have hydrophobic surfaces and in the absence of any proper surface coating, and the hydrophobic interactions between the NPs will cause them to aggregate and therefore, form large clusters, resulting in increased particle size and to reduce the surface energy.[20] Also magnetic particles lose their magnetism over time because bare iron oxide nanoparticles are easily oxidized in the air because of their high chemical activity, especially Fe_3O_4 and γ-Fe_2O_3 NPs.[21] Therefore, it is important to develop a proper protection strategy to chemically stabilize bare iron oxide nanoparticles against damage during or after the subsequent application. According to the surface characteristics of the functionalized nanoparticles, small molecules or surfactants functionalized Fe_3O_4 NPs can be simply divided to oil-soluble[22,23] or water-soluble.[24,25] For biomedical and many chemical applications, it is necessary to obtain water dispersible NPs.

3-Aminopropyltriethyloxysilane (APTES) agent was mostly employed for providing the amino group.[26] This agent is considered as a candidate for modification on the surface of Fe_3O_4 NPs. The high density of the surface functional group of NH_2, allowing for connecting to other targeting biomolecules and display well dispersion and stability in aqueous solvents, with retention of their physical characteristics of superparamagnetism with high saturation magnetization.[27] The functional group of NH_2 was reacted with other group and new catalysts such as Pd(II)–phosphine complexes,[28] Fe_3O_4-APTES-*N*-(2-aminoethyl)acrylamide,[29] Fe_3O_4–APTES–quinuclidine,[30] magnetic nanoparticles-crown,[31] polyaniline/Fe_3O_4,[32] Naproxen–APTES–Fe_3O_4,[33] Fe_3O_4–APTES–PEG[34] and Fe_3O_4–APTES–TCNP[35] were synthesized. Some of these catalysts like Fe_3O_4@APTES·Ac, Fe_3O_4@APTES·SAH,[36] Fe_3O_4–APTES·SO_3H[37,38] are acidic and Fe_3O_4@APTS–Py,[39] MNP–NMe_2, MNP–NH_2 (ref. 40) and Fe_3O_4@APTES@Ni(OH)$_2$ (ref. 41) are basic catalysts.

1,4-Dihydropyrdines have been reported as neurotropic,[42] anticancer,[43] antidiabetic[44] and glycoprotein inhibitors agents.[45] Various clinically used cardiovascular agents such as nicardipine, amlodipine, nifedipine, and other related derivatives are dihydropyridyl compounds effective in the treatment of hypertension.[46] Recently, studies showed that 1,4-dihydropyridine derivatives with lipophilic groups have considerable antitubercular activity against *M. tuberculosis* H37Rv.[47,48]

Department of Chemistry, Yasouj University, Yasouj 75918-74831, Iran. E-mail: manas@yu.ac.ir

1,8-Dioxooctahydroxanthenes are an important class of heterocyclic compounds. They have been found in a large number of naturally occurring molecules. Due to their wide-ranging therapeutic and biological properties such as antiviral,[49] antibacterial[50] and photodynamic therapy,[51] the synthesis of these compounds has attracted the attention of chemical and pharmaceutical researchers.

Bucricaine, Proflavine and Amsacrine are acridine derivatives and used topically for surface anesthesia of eye, bacteriostatic and antineoplastic respectively.[52,53] In addition, 1,8-dioxodecahydroacridines used as laser dyes, photoinitiators, antitumor, antimalaria, fungicidal and widely prescribed as calcium b-blockers.[54–59]

2-Pyridones attracted attention due to their applications as bioactive compounds for example as antibacterial,[60] antifungal,[61] as a promising class of HIV-1 non-nucleoside reverse transcriptase inhibitors,[62] antibiotics,[63] sedative[64] and cardiotonic agents.[65]

The imidazole derivatives especially triarylimidazole have many biological activities, for example, pharmaceuticals,[66] act as B-Raf kinase,[67] inhibitors of p38 MAP kinase,[68] antitumorals[69] and glucagon receptors.[70]

Therefore, the development of versatile and efficient procedures for the preparation of these types of compounds by using of new catalyst are active ongoing research area, and there will be a scope for further improvement toward low reaction times, improved yields and milder reaction conditions.

In this study, we want to report synthesis of new magnetically recoverable Brønsted acidic catalyst for the preparation of some new bulky heterocyclic compounds. For this purpose, we present a simple APTS-assisted hydrothermal approach to synthesizing APTS-coated Fe_3O_4 NPs with reactive surface amine groups. The surface-reactive amine groups of Fe_3O_4 NPs were further carboxylated by reacting with MAH (Fe_3O_4@APTES·MAH). The catalyst was characterized by X-ray

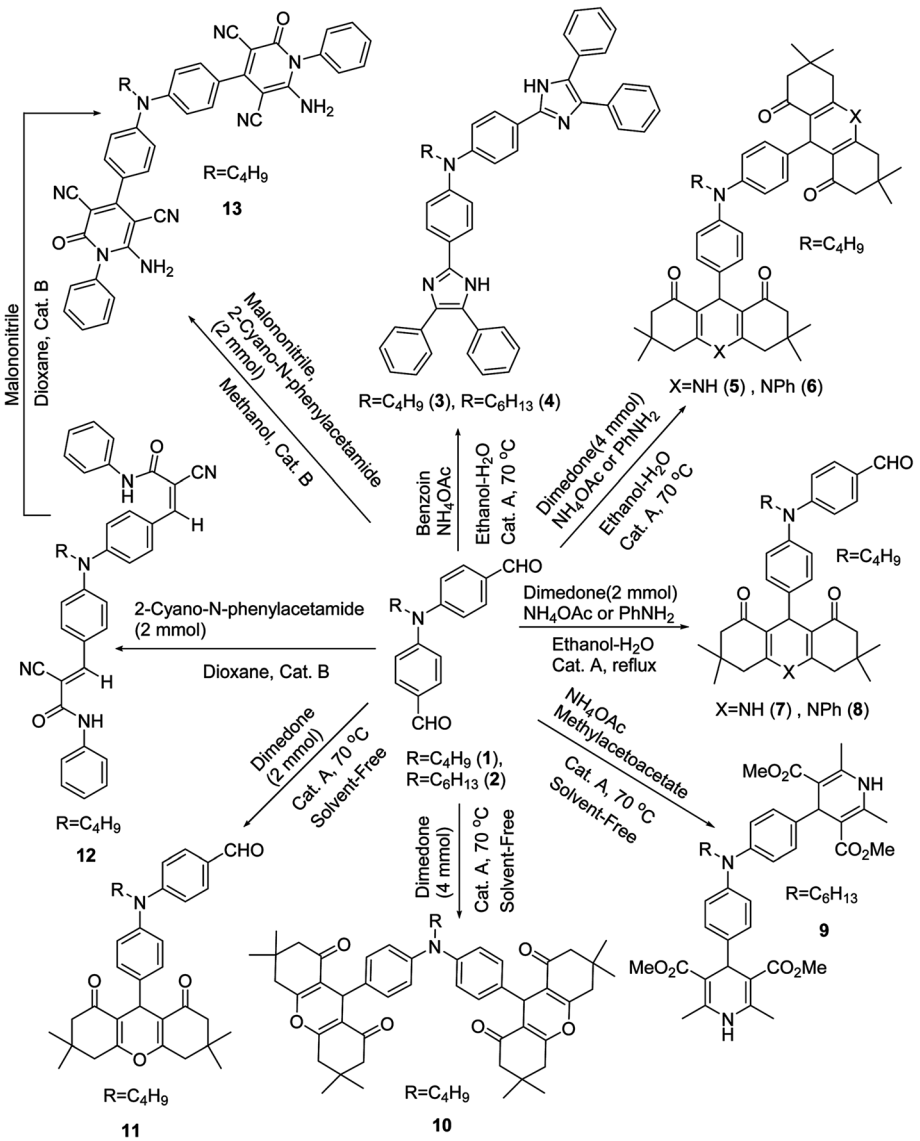

Scheme 1 Synthesis of new bulky heterocyclic compounds using 4,4-(alkylazanediyl)dibenzaldehyde as the substrate in the presence of Fe_3O_4@APTES·MAH NPs (Cat. A) or Fe_3O_4@APTES (Cat. B) as catalyst.

diffraction (XRD), transmission electron microscopy (TEM), Fourier transform infrared spectrometry (FT-IR), thermogravimetry analysis (TGA), dynamic light scattering (DLS) diagrams and vibrating scanning magnetometry (VSM). In the following some bulky heterocyclic compounds such as 1,4-dihydropyrdine, 1,8-dioxooctahydroxanthene, 1,8-dioxo-decahydroacridine, 2-pyridone and imidazole derivatives were prepared using Fe_3O_4@APTES or Fe_3O_4@APTES·MAH NPs as catalyst (Scheme 1).

Experimental

Chemicals were purchased from Merck or Aldrich. FT-IR spectra were recorded from KBr discs on a JASCO FT-IR-680. NMR spectra were taken with a Bruker 400 MHz Ultrashield spectrometer at 400 MHz (^{1}H) and 100 MHz (^{13}C) using $CDCl_3$ or DMSO-d_6 as the solvent with TMS as the internal standard. Thermal degradation of catalyst was carried out in the range 28–800 °C at a heating rate of 10 °C min^{-1} under nitrogen atmosphere using thermogravimetric analyzer-TG-209 F3, Netzsch, Germany. Energy dispersive X-ray spectroscopy analyses (EDAX) were carried out on a PHILIPS XL30, operated at a 20 kV accelerating voltage. The optical rotation was obtained with Jasco p-1030 polarimeter. Surface morphology and particle size were studied using a KYKY-EM-32000 SEM instrument and the X-ray diffraction (XRD) patterns of polymer and catalyst were recorded using an XRD (Bruker, D8 Advance, Rheinstetten, Germany) with a copper target at 40 kV and 35 mA and Cu Kα ($\lambda = 1.54$ Å) in the range of 10–80° at the speed of 0.05° min^{-1}. Magnetic characterization was carried out on a vibrating sample magnetometer (MDKB) at room temperature and the melting points were determined using an electrothermal digital melting point apparatus and are uncorrected. Reaction courses and product mixtures were monitored by thin layer chromatography (TLC).

Preparation of the catalyst

Fe_3O_4@APTES (500 mg) was dispersed in ethanol (5 mL) using ultrasonic bath for 30 min. Subsequently, maleic anhydride (1.47 g) was dissolved in DMSO (5 mL) and added dropwise over a period of 20 min at room temperature under vigorous stirring. The mixture was stirred for 24 h and the functionalized nanoparticles were separated by centrifugation. Then the solid catalyst was washed with dry CH_2Cl_2 and was subsequently separated using centrifugation and finally dispersed in ethanol.

Synthesis of compounds 3 and 4

A mixture of ammonium acetate (8 mmol, 0.62 g) and benzoin (2 mmol, 0.42 g) was dissolved in ethanol–water mixture (8 mL, 1 : 1, v/v) and to the reaction mixture 1 mmol of dialdehyde (**1**, 0.281 g, or **2**, 0.309 g) and Fe_3O_4@APTES·MAH NPs (0.08 g) were added. Then, the reaction mixture was heated at 70 °C for 130 or 145 min (**3** or **4**, respectively). The reaction mixture was cooled to room temperature and solid catalyst separated by a magnet. The reaction mixture was poured into ice-water (5 mL) to obtain the solid. Then it was collected by filtration, washed with water and dried to give the pure product.

***N*-Butyl-4-(4,5-diphenyl-1*H*-imidazol-2-yl)-*N*-(4-(4,5-diphenyl-1*H*-imidazol-2-yl)phenyl)aniline (3).** Pale yellow solid; mp: 86–88 °C; yield: 78% (0.49 g); IR (KBr, cm^{-1}): 3316, 3062, 2925, 2885, 1660, 1592, 1450, 1322, 1211, 1172; ^{1}H NMR (400 MHz, $CDCl_3$) δ (ppm): 9.91 (2H, s, N–H), 8.00 (12H, d, $J = 7.2$ Hz, Ar-H), 7.69 (4H, t, $J = 7.4$ Hz, Ar-H), 7.54 (12H, t, $J = 7.7$ Hz, Ar-H), 3.87 (2H, t, $J = 7.5$ Hz, N–CH_2), 1.70–1.59 (2H, m, CH_2), 1.42–1.27 (2H, m, CH_2), 0.97 (3H, t, $J = 7.3$ Hz, CH_3); ^{13}C NMR (100 MHz, $CDCl_3$) δ (ppm): 194.61, 134.93, 132.99, 131.61, 130.10, 130.06, 129.94, 129.05, 128.65, 120.73, 54.90, 45.75, 41.65, 10.70; anal. calcd $C_{46}H_{39}N_5$: C 83.48, H 5.94, N 10.58; found: C 83.29, H 5.90, N 10.53.

4-(4,5-Diphenyl-1*H*-imidazol-2-yl)-*N*-(4-(4,5-diphenyl-1*H*-imidazol-2-yl)phenyl)-*N*-hexylaniline (4). Brown solid; mp: 140–142 °C; yield: 68% (0.47 g); IR (KBr, cm^{-1}): 3324, 3059, 2925, 2859, 1670, 1602, 1457, 1320, 1218, 1180; ^{1}H NMR (400 MHz, $CDCl_3$) δ (ppm): 10.31 (2H, s, N–H), 7.96 (4H, t, $J = 8.4$ Hz, Ar-H), 7.54 (8H, d, $J = 7.97$ Hz, Ar-H), 7.34 (12H, t, $J = 7.84$ Hz, Ar-H), 7.10 (4H, t, $J = 7.35$ Hz, Ar-H), 3.79 (2H, t, $J = 7.7$ Hz, N–CH_2), 1.76–1.68 (2H, m, CH_2), 1.36–1.25 (6H, m, $3CH_2$), 0.90 (3H, t, $J = 6.8$ Hz, CH_3); ^{13}C NMR (100 MHz, $CDCl_3$) δ (ppm): 189.78, 140.85, 136.46, 132.42, 131.06, 130.25, 130.05, 127.84, 120.11, 116.80, 51.54, 31.99, 31.50, 26.56, 22.63, 14.02; anal. calcd $C_{48}H_{43}N_5$: C 83.57, H 6.28, N 10.15; found: C 83.41, H 6.24, N 10.09.

Synthesis of compounds 5 and 6

A mixture of 4,4-(butylazanediyl)dibenzaldehyde (**1**, 1 mmol, 0.28 g), 5,5-dimethyl-1,3-cyclohexanedione (4 mmol, 0.56 g), Fe_3O_4@APTES·MAH NPs (0.06 g) and 2 mmol amine (ammonium acetate, 0.15 g or aniline, 0.19 g) into a 25 mL round bottomed flask was heated at 70 °C in ethanol–water (8 mL, v/v = 1) for 55 or 48 min (for compounds **5** or **6**, respectively). The reaction mixture was cooled to room temperature and solid catalyst separated by a magnet. The reaction mixture was concentrated on a rotary evaporator under reduced pressure and the obtained solid product was recrystallized in ethanol.

9,9-((Butylazanediyl)bis(1,4-phenylene))bis(3,3,6,6-tetramethyl-3,4,6,7,9,10-hexahydroacridine-1,8(2*H*,5*H*)-dione) (5). Yellow solid; mp: 231–233 °C; yield: 80% (0.58 g); IR (KBr, cm^{-1}): 3428, 2956, 2869, 1631, 1612, 1506, 486, 1222; ^{1}H NMR (400 MHz, DMSO-d_6) δ (ppm): 8.81 (2H, s, NH), 7.12 (4H, d, $J = 8.5$, Ar-H), 6.73 (4H, d, $J = 8.5$, Ar-H), 5.03 (2H, s, 2 × CH), 3.70 (2H, t, $J = 6.5$ Hz, N–CH_2), 2.33 (4H, d, 2 × CH_2, $J = 18$ Hz), 2.21 (4H, d, 2 × CH_2, $J = 16.3$ Hz), 2.06 (8H, s, 4 × CH_2), 1.54–1.51 (2H, m, CH_2), 1.29–1.24 (2H, m, CH_2), 1.09 (12H, s, 4 × CH_3), 1.00 (12H, s, 4 × CH_3), 0.88 (3H, t, $J = 5.5$ Hz); ^{13}C NMR (100 MHz, $CDCl_3$) δ (ppm): 198.68 (C═O), 151.39 (C═C), 147.07, 128.43, 120.26, 119.96 (Ar-C), 115.19 (C═C), 60.42 (4 × CH_2), 58.50 (CH_2), 50.79 (4 × CH_2), 32.74 (2 × CH), 29.43 (4 × $C(CH_3)_2$), 27.33 (CH_2), 21.08 (8 × CH_3), 18.45 (CH_2), 14.14 (CH_3); anal. calcd $C_{50}H_{61}N_3O_4$: C 78.19, H 8.01, N 5.47, O 8.33; found: C 78.03, H 7.95, N 5.43.

9,9-((Butylazanediyl)bis(1,4-phenylene))bis(3,3,6,6-tetramethyl-10-phenyl-3,4,6,7,9,10-hexahydroacridine-1,8(2*H*,5*H*)-dione) (6). Pale yellow solid; mp: 169–171 °C; yield: 77% (0.71 g);

IR (KBr, cm^{-1}): 3062, 2960, 1596, 1571, 1494, 1243; ^1H NMR (400 MHz, $CDCl_3$) δ (ppm): 7.61 (2H, d, $J = 8.78$ Hz, Ar-H), 7.86 (4H, t, $J = 7.86$ Hz, Ar-H), 7.18 (4H, d, $J = 7.74$ Hz, Ar-H), 7.13 (4H, t, $J =$ 7.35 Hz, Ar-H), 6.68–6.64 (4H, m, Ar-H), 5.31 (2H, s, CH), 3.69 (2H, t, $J = 7.67$ Hz, N–CH_2), 2.38 (8H, s, 4 × CH_2), 2.05 (8H, s, 4 × CH_2), 1.32–1.18 (4H, m, 2 × CH_2), 1.03 (24H, s, 8 × CH_3), 0.87 (3H, t, $J = 7.74$ Hz, CH_3), ^{13}C NMR (100 MHz, $CDCl_3$) δ (ppm): 195.36 (C═O), 160.01 (C═C), 139.14, 139.04, 129.17, 124.29, 122.92, 122.87, 122.80, 122.75 (Ar-C), 110.73 (–C═C), 50.12 (4 × CH_2), 41.99 (CH_2), 41.93 (CH_2), 32.25 (4 × CH_2), 27.92 (2 × CH), 29.55 (4 × $C(CH_3)_2$), 29.09 (CH_2), 28.03 (8 × CH_3), 20.07 (CH_2), 13.85 (CH_3); anal. calcd $C_{62}H_{69}N_3O_4$: C 80.92, H 7.56, N 4.57, O 6.95; found: C 80.79, H 7.53, N 4.54.

Synthesis of compounds 7 and 8

Into a 25 mL round bottomed flask, a mixture of 4,4′-(butylazanediyl)dibenzaldehyde **1** (1 mmol, 0.28 g), 5,5-dimethyl-1,3-cyclohexanedione (2 mmol, 0.28 g), Fe_3O_4@APTES·MAH NPs (0.03 g) and 1 mmol amine (ammonium acetate, 0.08 g or aniline, 0.09 g) was refluxed in ethanol–water mixture (8 ml, v/v = 1) for 40 or 45 min (for compounds **7** or **8**, respectively). The reaction mixture was cooled to room temperature and solid catalyst separated by a magnet. The reaction mixture was concentrated using a rotary evaporator under reduced pressure and the solid product was recrystallized in ethanol.

4-(Butyl(4-(3,3,6,6-tetramethyl-1,8-dioxo-1,2,3,4,5,6,7,8,9,10-decahydroacridin-9-yl)phenyl)amino)benzaldehyde (7). Pale yellow solid; mp: 161–163 °C; yield: 68% (0.36 g); $[\alpha]_D^{20} = +109.2°$ ($c = 0.21$ g mL^{-1}, $CHCl_3$); IR (KBr, cm^{-1}): 3066, 3028, 2956, 2871, 1643, 1608, 1608, 1484, 1220; ^1H NMR (400 MHz, DMSO-d_6) δ (ppm): 9.71 (1H, s, CHO), 8.32 (1H, s, NH), 7.81 (2H, d, $J =$ 8.1, Ar-H), 7.08 (2H, d, $J = 8.5$, Ar-H), 6.91 (2H, d, $J = 8.1$, Ar-H), 6.40 (2H, d, $J = 8.5$, Ar-H), 4.73 (1H, s, CH), 4.14 (1H, q, $J = 5.3$ Hz, N–CH_2), 3.75 (1H, q, $J = 7.6$ Hz, N–CH_2), 2.52 (2H, d, CH_2, $J =$ 18 Hz), 2.45 (2H, d, CH_2, $J = 16.3$ Hz), 2.16 (4H, s, 2 × CH_2), 1.56–1.48 (2H, m, CH_2), 1.34–1.26 (2H, m, CH_2), 1.10 (6H, s, 2 × CH_3), 1.00 (6H, s, 2 × CH_3), 0.90 (3H, t, $J = 5.5$ Hz); ^{13}C NMR (100 MHz, DMSO-d_6) δ (ppm): 194.22 (C═O), 191.05 (–C═O, aldehyde), 149.54 (C═C), 152.14, 148.65, 138.12, 130.85, 128.76, 127.29, 119.62, 113.81 (Ar-C), 112.80 (C═C), 50.12 (2 × CH_2), 46.16 (CH_2), 40.86 (2 × CH_2), 39.71 (CH), 31.85 (2 × $C(CH_3)_2$), 29.09 (CH_2), 28.03 (4 × CH_3), 20.07 (CH_2), 13.85 (CH_3); anal. calcd $C_{34}H_{40}N_2O_3$: C 77.83, H 7.68, N 5.34, O 9.15; found: C 77.71, H 7.63, N 5.30.

4-(Butyl(4-(3,3,6,6-tetramethyl-1,8-dioxo-10-phenyl-1,2,3,4,5,6,7,8,9,10-decahydroacridin-9-yl)phenyl)amino)benzaldehyde (8). Orange solid; mp: 106–109 °C; yield: 70% (0.42 g); $[\alpha]_D^{20} = +71.5°$ ($c = 0.33$ g mL^{-1}, $CHCl_3$); IR (KBr, cm^{-1}): 2956, 2923, 2869, 1642, 1592, 1508, 1448, 1249; ^1H NMR (400 MHz, $CDCl_3$) δ (ppm): 9.74 (1H, s, CHO), 7.66 (2H, d, $J = 8.8$ Hz, Ar-H), 7.38–7.17 (4H, m, Ar-H), 7.12 (1H, d, $J = 5.5$ Hz, Ar-H), 6.96 (2H, d, $J =$ 8.5, Ar-H), 6.88 (2H, d, $J = 8.6$ Hz, Ar-H), 6.70 (2H, d, $J = 8.5$ Hz, Ar-H), 5.49 (1H, s, CH), 3.71 (1H, t, $J = 7.6$ Hz, N–CH_2), 3.62 (1H, t, $J = 7.6$ Hz, N–CH_2), 2.45 (2H, d, $J = 13.4$ Hz, CH_2), 2.38 (2H, d, $J = 16.0$ Hz, CH_2), 2.26 (4H, s, 2 × CH_2), 1.39–1.33 (2H, m, CH_2), 1.28–1.24 (2H, m, CH_2), 1.14 (6H, s, 2 × CH_3), 1.11 (6H, s, 2 × CH_3), 0.94 (3H, t, $J = 6.7$ Hz, CH_3); ^{13}C NMR (100 MHz, $CDCl_3$) δ (ppm): 190.23 (C═O), 189.28 (–C═O, aldehyde), 160.02 (C═C), 145.93, 131.79, 130.16, 129.42, 128.51, 127.59, 127.20, 125.62, 123.84, 120.51, 115.73, 115.15 (Ar-C), 113.25 (C═C), 50.33 (2 × CH_2), 47.08 (CH_2), 46.47 (2 × CH_2), 43.76 (CH), 31.37 (2 × $C(CH_3)_2$), 29.75 (CH_2), 27.38 (4 × CH_3), 20.31 (CH_2), 13.96 (CH_3); anal. calcd $C_{40}H_{44}N_2O_3$: C 79.97, H 7.38, N 4.66, O 7.99; found: C 79.83, H 7.35, N 4.64.

Synthesis of compound 9

Into a 25 mL round bottomed flask, the mixture of 4,4′-(hexylazanediyl)dibenzaldehyde **2** (1 mmol, 0.31 g), ammonium acetate (1.5 mmol, 0.12 g) and methyl acetoacetate (4 mmol, 0.46 g) and Fe_3O_4@APTES·MAH NPs (0.05 g) was heated at 70 °C under solvent free conditions. After completion of the reaction (40 min), the mixture was cooled to room temperature and then ethanol (5 mL) was added to the resulting mixture and catalyst separated by a magnet. After evaporation of solvent, the solid product was filtered and recrystallized from ethanol to give the pure products.

Tetramethyl 4,4′-((hexylazanediyl)bis(4,1-phenylene))bis(2,6-dimethyl-1,4-dihydropyridine-3,5-dicarboxylate) (9). Brown solid; mp: 92–94 °C; yield: 86% (0.61 g); IR (KBr, cm^{-1}): 3338, 3091, 2950, 2927, 2854, 1697, 1506, 1488, 1432, 1305, 1216, 1118, 1097; ^1H NMR (400 MHz, $CDCl_3$) δ (ppm): 7.11 (4H, d, $J =$ 8.5 Hz, Ar-H), 6.78 (4H, d, $J = 8.5$ Hz, Ar-H), 5.83 (2H, s, N–H), 4.95 (2H, s, CH), 3.68 (12H, s, 4 × O–CH_3), 3.57 (2H, t, $J = 7.7$ Hz, N–CH_2), 2.34 (12H, s, 4 × CH_3), 1.61 (2H, brs, CH_2), 1.24–1.36 (6H, m, 3CH_2), 0.88 (3H, t, $J = 6.6$ Hz, CH_3); ^{13}C NMR (100 MHz, $CDCl_3$) δ (ppm): 168.27, 146.32, 144.05, 139.89, 128.24, 120.24, 104.03, 52.36, 51.02, 38.32, 31.66, 29.71, 26.75, 22.70, 19.56, 14.05; anal. calcd $C_{40}H_{49}N_3O_8$: C 68.65, H 7.06, N 6.00, O 18.29; found: C 68.50, H 7.02, N 5.96.

Synthesis of compounds 10 and 11

A mixture of 4,4′-(butylazanediyl)dibenzaldehyde **1** (1 mmol, 0.28 g), 5,5-dimethyl-1,3-cyclohexanedione (4 mmol 0.56 g for **10**; 2 mmol 0.28 g for **11**) and Fe_3O_4@APTES·MAH NPs (0.08 g for **10**; 0.04 g for **11**) into a 25 mL round bottomed flask, was heated in an oil bath at 70 °C under solvent-free conditions. After completion of the reaction (35 min, **10**; 45 min, **11**) the resulting solid was cooled and dichloromethane (5 mL) added and stirred for a few minutes. Then, the catalyst was separated by magnet. The remained solution was kept overnight and the crude product recrystallized from ethanol to afford the pure product.

9,9′-((Butylazanediyl)bis(1,4-phenylene))bis(3,3,6,6-tetramethyl-3,4,5,6,7,9-hexahydro-1*H*-xanthene-1,8(2*H*)-dione) (10). Green-blue solid; mp: 225–227 °C; yield: 82% (0.63 g); IR (KBr, cm^{-1}): 2958, 2930, 1665, 1623, 1509, 1359, 1197, 1137; ^1H NMR (400 MHz, $CDCl_3$) δ (ppm): 7.09 (4H, d, $J = 8.5$ Hz, Ar-H), 6.76 (4H, d, $J = 8.5$ Hz, Ar-H), 4.70 (2H, s, CH), 3.53 (2H, t, $J = 7.5$ Hz, N–CH_2), 2.48 (8H, s, 4 × CH_2), 2.23 (8H, s, 4 × CH_2), 1.53 (2H, m, CH_2), 1.26 (2H, m, CH_2), 1.11 (12H, s, 4 × CH_3), 1.01 (12H, s, 4 × CH_3), 0.88 (3H, t, $J = 7.3$ Hz, CH_3); ^{13}C NMR (100 MHz, $CDCl_3$) δ (ppm): 196.57 (C═O), 162.13 (C═C), 146.2, 136.4,

128.8, 120.31 (Ar-C), 115.83 (C═C), 50.83 (4 × CH_2), 40.87 (CH_2), 32.23 (4 × CH_2), 30.77 (2 × CH), 29.55 (4 × $C(CH_3)_2$), 29.20 (CH_2), 27.50 (8 × CH_3), 20.20 (CH_2), 13.91 (CH_3); anal. calcd $C_{50}H_{59}NO_6$: C 77.99, H 7.72, N 1.82, O 12.47; found: C 77.83, H 7.68, N 1.80.

4-(Butyl(4-(3,3,6,6-tetramethyl-1,8-dioxo-2,3,4,5,6,7,8,9-octahydro-1*H*-xanthen-9- yl)phenyl)amino)benzaldehyde (11). Orange solid; mp: 72–74 °C; yield: 69% (0.36 g); $[\alpha]_D^{20} = +23.5°$ (c = 0.3 g mL^{-1}, $CHCl_3$); IR (KBr, cm^{-1}): 2963, 2935, 2871, 1728, 1663, 1623, 1509, 1359, 1195, 1145; ^{1}H NMR (400 MHz, $CDCl_3$) δ (ppm): 9.91 (1H, s, CHO), 7.81 (2H, d, J = 8.4 Hz, Ar-H), 7.09 (2H, d, J = 8.5 Hz, Ar-H), 6.91 (2H, d, J = 8.5, Ar-H), 6.76 (2H, d, J = 8.5 Hz, Ar-H), 4.73 (1H, s, CH), 3.53 (2H, t, J = 7.5 Hz, N–CH_2), 2.48 (4H, s, 2 × CH_2), 2.19 (4H, s, 2 × CH_2), 1.51 (2H, m, CH_2), 1.25 (2H, m, CH_2), 1.11 (6H, s, 2 × CH_3), 1.01 (6H, s, 2 × CH_3), 0.88 (3H, t, J = 7.3 Hz, CH_3); ^{13}C NMR (100 MHz, $CDCl_3$) δ (ppm): 201.20 (–C═O, aldehyde), 197.54 (C═O), 162.95 (C═C), 148.65, 138.12, 130.85, 128.65, 127.29, 113.81(Ar-C), 112.80 (C═C), 50.05 (2 × CH_2), 46.10 (CH_2), 40.86 (2 × CH_2), 37.71 (CH), 31.85 (2 × $C(CH_3)_2$), 29.09 (CH_2), 28.18 (4 × CH_3), 20.07 (CH_2), 13.83 (CH_3); anal. calcd $C_{34}H_{39}NO_4$: C 77.68, H 7.48, N 2.66, O 12.17; found: C 77.52, H 7.44, N 2.63.

Synthesis of compound 12

A solution of 2-cyano-*N*-phenylacetamide (**14**, 2 mmol, 0.32 g) and 4,4′-(butylazanediyl)dibenzaldehyde (**1**, 1 mmol, 0.28 g) in 1,4-dioxane (10 mL) was divided into two equal parts. Into the first part in a 25 mL round bottomed flask, Fe_3O_4@APTES (0.1 g) was added and heated at 70 °C for 7 h, cooled to room temperature and solid catalyst was separated by a magnet. The residual solution was poured into the mixture of ice-water containing two drops of HCl and the solid product was collected by filtration and recrystallized from 1,4-dioxane. Into the second part of the solution, triethylamine (0.2 mL) was added and the reaction mixture was heated under reflux conditions for 4 h. The reaction mixture was poured into the mixture of ice-water and two drops of HCl. The solid product was collected by filtration and recrystallized from 1,4-dioxane.

3,3′-((Butylazanediyl)bis(1,4-phenylen))bis(2-cyano-*N*-phenylacrylamide) (12). Orange solid, mp: 140–142 °C; yields: part 1, 0.43 g, 75%; part 2, 0.50 g, 88%; IR (KBr, cm^{-1}): 3328, 3056, 2956, 2927, 2206, 1675, 1590, 1535, 1504, 1438, 1313, 1180, 827; ^{1}H NMR (400 MHz, $CDCl_3$) δ (ppm): 9.85 (1H, s, N–H), 9.82 (1H, s, N–H), 8.28 (1H, s, CH═C), 8.26 (1H, s, CH═C), 7.91–7.86 (4H, dd, J_1 = 11.0 Hz, J_2 = 8.8 Hz, Ar-H), 7.76 (4H, dd, J_1 = 14.0 Hz, J_2 = 8.7 Hz, Ar-H), 7.32 (4H, t, J = 7 Hz, Ar-H), 7.11 (4H, dd, J_1 = 10.1 Hz, J_2 = 8.9 Hz), 7.03 (2H, d, J = 8.8 Hz), 3.79 (2H, t, J = 7.7 Hz, N–CH_2), 1.61–1.66 (2H, m, CH_2), 1.31–1.34 (2H, m, CH_2), 0.89 (3H, t, J = 5.8 Hz, CH_3); ^{13}C NMR (100 MHz, $CDCl_3$) δ (ppm): 190.55, 152.66, 133.04, 131.61, 129.21, 125.94, 121.94, 120.97, 120.73, 120.42, 119.79, 52.33, 29.67, 20.21, 13.84; anal. calcd $C_{36}H_{31}N_5O_2$: C, 76.44; H, 5.52; N, 12.38; O, 5.66; found: C 76.30, H 5.49, N 12.33.

Synthesis of compound 13

Method A. A mixture of 4,4′-(butylazanediyl)dibenzaldehyde **1** (1 mmol, 0.28 g), 2-cyano-*N*-phenylacetamide (**14**, 2 mmol, 0.32 g), malononitrile (2 mmol, 0.13 g) in methanol (10 mL) was divided into two equal parts. Into the first part in a 25 mL round bottomed flask, suspension of Fe_3O_4@APTES (0.1 g) in methanol (5 mL) was added and refluxed for 8 h. The reaction mixture was cooled to room temperature and solid catalyst separated by a magnet. The reaction mixture was concentrated under reduced pressure and then water (5 mL) was added. The obtained solid product was filtered off, dried and recrystallized from ethanol.

Into the second part of the above mixture, catalytic amount of triethylamine (0.2 mL) in methanol (10 mL) was added and heated under reflux conditions for 4 h. The reaction mixture was kept at room temperature for 1 h and then 5 mL cold water was added. Then the solid product was isolated and recrystallized from ethanol.

Method B. A solution of compound **12** (1 mmol, 0.57 g) and malononitrile (2 mmol, 0.13 g) in 1,4-dioxane (15 mL) and dimethylformamide (7 mL) was divided into two equal parts. In a 25 mL round bottomed flask into the first part of the solution, Fe_3O_4@APTES (0.1 g) was added and heated at 70 °C for 9 h. The reaction mixture was cooled to room temperature and solid catalyst separated by a magnet and the residual was poured into ice/water containing 2 drops of hydrochloric acid. The solid products were collected and recrystallized from 1,4-dioxane.

Into second part of the solution, triethylamine (0.2 mL) was added and heated under reflux for 5 h. Then the mixture was cooled and poured into ice/water containing 2 drops of concentrated HCl. The solid products were collected and recrystallized from 1,4-dioxane (Scheme 4).

4,4′-((Butylazanediyl)bis(4,1-phenylene))bis(6-amino-2-oxo-1-phenyl-1,2-dihydropyridine-3,5-dicarbonitrile) (13). Pale brown solid; mp: 154–157 °C; yields: method A: part 1, 0.313 g 45%; part 2, 0.502 g 72%; method B: part 1, 0.278 g 40%; part 2, 0.453 g 65%; IR (KBr, cm^{-1}): 3270, 3208, 3052, 2956, 2260, 2211, 1668, 1600, 1508, 1488, 1392, 1187; ^{1}H NMR (400 MHz, $CDCl_3$) δ (ppm): 7.72 (4H, brs, 2NH_2), 7.53 (8H, d, J = 7.9 Hz, Ar-H), 7.40 (8H, t, J = 7.8 Hz, Ar-H), 7.23 (2H, t, J = 7.3, Ar-H), 3.76 (2H, t, J = 7.0 Hz, N–CH_2), 1.32–1.37 (2H, m, CH_2), 1.16–1.23 (2H, m, CH_2), 0.89 (3H, t, J = 7.0 Hz, CH_3); ^{13}C NMR (100 MHz, $CDCl_3$) δ (ppm): 160.99, 149.95, 149.88, 147.16, 138.34, 130.32, 128.89, 128.62, 123.85, 120.53, 119.16, 119.06, 115.93, 74.76, 45.64, 26.71, 19.52, 13.79; anal. calcd $C_{42}H_{31}N_9O_2$: C 72.71, H 4.50, N 18.17, O 4.61; found: C 72.58, H 4.48, N 18.10.

Results and discussion

Because of the high surface energy, the naked Fe_3O_4 nanoparticles are generally unstable and aggregate easily and alter magnetic properties. In addition, Fe_3O_4 nanoparticles are highly susceptible to be oxidized to γ-Fe_2O_3 nanoparticles in the presence of oxygen.[71] To overcome such limitations, various surface modification methods have been developed to modify the surface of naked Fe_3O_4 nanoparticles.[72,73] With proper surface modification, the stability and dispersity of Fe_3O_4 nanoparticles could be improved, and the oxidation process from Fe_3O_4 nanoparticles to γ-Fe_2O_3 nanoparticles could be greatly slowed down.

Fe_3O_4 MNPs were prepared using procedure described in the literature[74] and subsequently were coated with 3-aminopropyltriethoxysilane to achieve amino functionalized magnetic nanoparticles Fe_3O_4@APTES MNPs.[26]

MAH was used for further modification of Fe_3O_4@APTES MNPs. A very useful property of the MAH moieties is their spontaneous reactivity towards primary amines, which can be easily modified surface NPs. Each MAH ring yields a free carboxylic group after reaction with the amine. This was resulting in NPs with increased stability, *e.g.* in a biological environment.[75] For preparation of Fe_3O_4@APTES·MAH magnetic nanoparticles, the dispersed Fe_3O_4@APTES in ethanol was dropwise added to a solution of maleic anhydride in DMSO and the functionalized nanoparticles were separated using centrifugation (Scheme 2). MAH contains carboxylic acid groups so, it can activate the electrophilic compounds by hydrogen bonding and lone pairs.

As can be seen in Scheme 2, Fe_3O_4 as a Lewis acid and the free carboxyl groups on the surface of MAH provide the solid acid catalyst and play a significant role in increasing the electrophilic character of the dialdehyde and so can activate the carbonyl group of aldehyde to decrease the energy of transition state for the nucleophilic attack. Considering the superparamagnetic properties and the ease chemical modification, this solid acid catalyst can use in many organic reactions as a solid acidic catalyst.

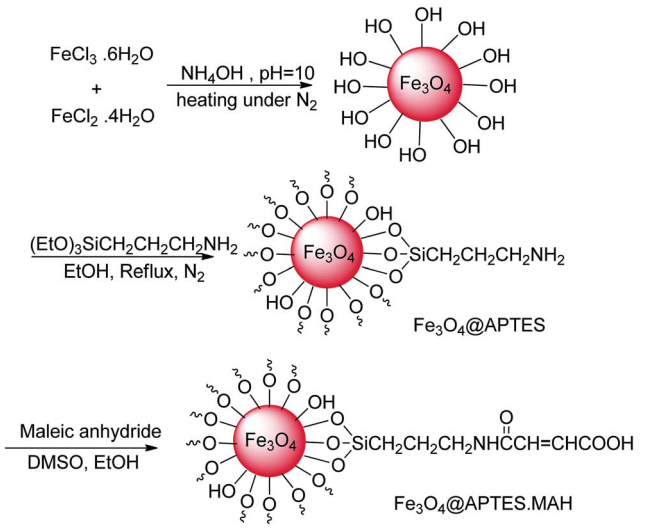

Scheme 2 Synthesis route for the maleic anhydride coated magnetite nanoparticles.

Characterization and stability of the catalyst

Fig. 1 indicates the FT-IR spectra of the unmodified Fe_3O_4 nanoparticles (Fig. 1a), modified Fe_3O_4 nanoparticles by 3-aminopropyltriethoxysilane (Fig. 1b) and Fe_3O_4@APTES·MAH (Fig. 1c). The corresponding absorption bands of these compounds are listed in Table 1. The sharp and revealing band at around 579–585 cm^{-1} are relates to Fe–O bond.[76] The bands around 1633 and 3438 cm^{-1} are due to the hydroxyl groups on the Fe_3O_4 nanoparticles are observed in Fig. 1a. The Fe–O stretching vibration near 580 cm^{-1}, O–H stretching vibration near 3428 cm^{-1}, O–H deformed vibration near 1633 cm^{-1}, Si–O stretching at 1029 and 1122 cm^{-1}, $-CH_2$ stretching at 2852 cm^{-1} were observed for Fe_3O_4@APTES (Fig. 1b). The band at 3428 cm^{-1} was probably attributed to the free amino groups, which is overlapped by the O–H stretching vibration (Fig. 1b). These results provided the evidence that the γ-aminopropyltriethyoxysilane was successfully attached to the surface of Fe_3O_4 nanoparticles.[77] Fig. 1c shows the FT-IR spectrum of Fe_3O_4@APTES·MAH nanoparticles. The main characteristics

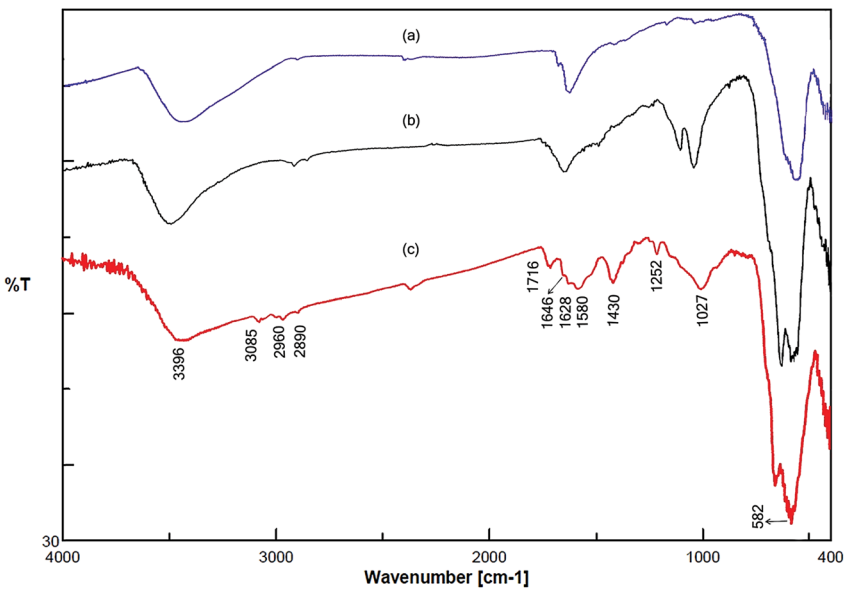

Fig. 1 FT-IR spectra of unmodified Fe_3O_4 nanoparticles (a), modified Fe_3O_4 nanoparticles by γ-aminopropyltriethyoxysilane (b) and Fe_3O_4@APTES·MAH (c).

Table 1 EDAX quantification element normalized

		Fe_3O_4@APTES		Fe_3O_4@APTES·MAH	
Element	Series	Wt%	At%	Wt%	At%
Carbon	K-series	9.13	19.48	12.14	23.86
Nitrogen	K-series	1.47	2.70	1.38	2.32
Oxygen	K-series	31.52	50.50	34.62	51.10
Silicon	K-series	1.72	1.57	1.94	1.63
Iron	K-series	56.16	25.75	49.92	21.09

bands are assigned as follow: the band at 3396 cm^{-1} is attributable to N–H stretching mode, which is overlapped by the O–H stretching vibration, –C═CH and $–CH_2$ stretching at 3085 and 2890 cm^{-1} respectively, C═O stretching mode for acid and amide at 1716 and 1646 cm^{-1} and C═C stretching vibration at 1628 cm^{-1}. The bands around 1430 and 1252 cm^{-1} have been attributed to C–N and C–O stretching mode for amide and acid. The bands at 1027 and 582 cm^{-1} are assigned to the oxygen–silicon and oxygen–iron stretching vibration.

The XRD patterns of Fe_3O_4@APTES and Fe_3O_4@APTES·MAH nanoparticles (Fig. 2) indicate their cubic structures. The position and relative intensities of all peaks confirm well with standard XRD pattern of Fe_3O_4 (Fig. 3) indicating retention of the crystalline cubic spinel structure during functionalization of Fe_3O_4 nanomagnetic. The XRD patterns of the particles show six characteristic peaks reveal a cubic iron oxide phrase ($2\theta = 30.1$, 35.5, 43.0, 53.5, 57.2, 62.7, 73.9). As it can be seen in Fig. 2, the following peak signals at (220), (311), (400), (422), (511), (440) and (533) planes of Fe_3O_4 crystals, respectively, which coincides with JCPD 00-001-1111 standard. The size of Fe_3O_4@APTES and Fe_3O_4@APTES·MAH was also determined by X-ray line broad using the Debye–Scherrer formula given as $D = 0.9\lambda/\beta \cos\theta$, where D is the average crystalline size, λ the X-ray wavelength used (1.5406 Å for Cu Kα) and β is the angular line width at half maximum intensity and θ is the Bragg's angle. The average size of Fe_3O_4@APTES and Fe_3O_4@APTES·MAH nanoparticles for $2\theta = 35.5844°$ was respectively estimated around 17.7 nm and 20.2 nm, due to the agglomeration of Fe_3O_4 inside nanospheres and surface growth of amine and acid on the shell.

Fig. 4 shows the morphology of Fe_3O_4@APTES·MAH as obtained by scanning electron microscopy (SEM) micrograph (a), transmission electron microscopy (TEM) (b), and dynamic light scattering (DLS) diagrams (c).

As shown in Fig. 4a and b, the TEM and SEM images show that Fe_3O_4@APTES·MAH nanoparticles were spherical with a mean diameter of 20 nm, with uniform size, and showed good dispersity. Also, it shows spherical morphology after being coated Fe_3O_4 with APTES shell and maleic anhydride. In short the SEM and TEM images indicate the successful coating of the magnetic Fe_3O_4 particles.

The particle size of the synthesized Fe_3O_4@APTES·MAH nanoparticles was also determined using DLS measurement technique. Dynamic light scattering is a technique for characterizing the size of colloidal dispersions which utilizes the illumination of a suspension of particles or molecules undergoing Brownian motion by a laser beam. The technique of dynamic light scattering has been widely employed for sizing magnetic nanoparticles in liquid phase.[78,79]

Fig. 4c shows the typical DLS size distribution graph by intensity of the synthesized Fe_3O_4@APTES·MAH. The size distribution by intensity shows an average width peak in the range 20 to 80 nm. The average size of Fe_3O_4@APTES·MAH is

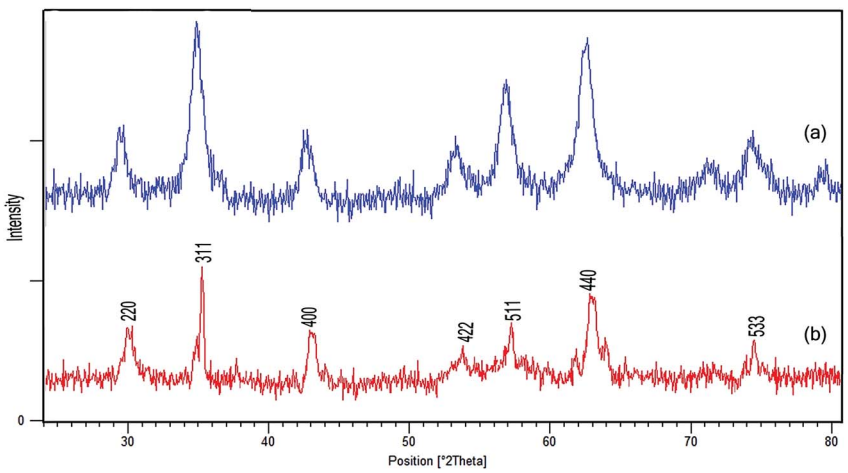

Fig. 2 The X-ray diffraction pattern of (a) Fe_3O_4@APTES NPs and (b) Fe_3O_4@APTES·MAH NPs.

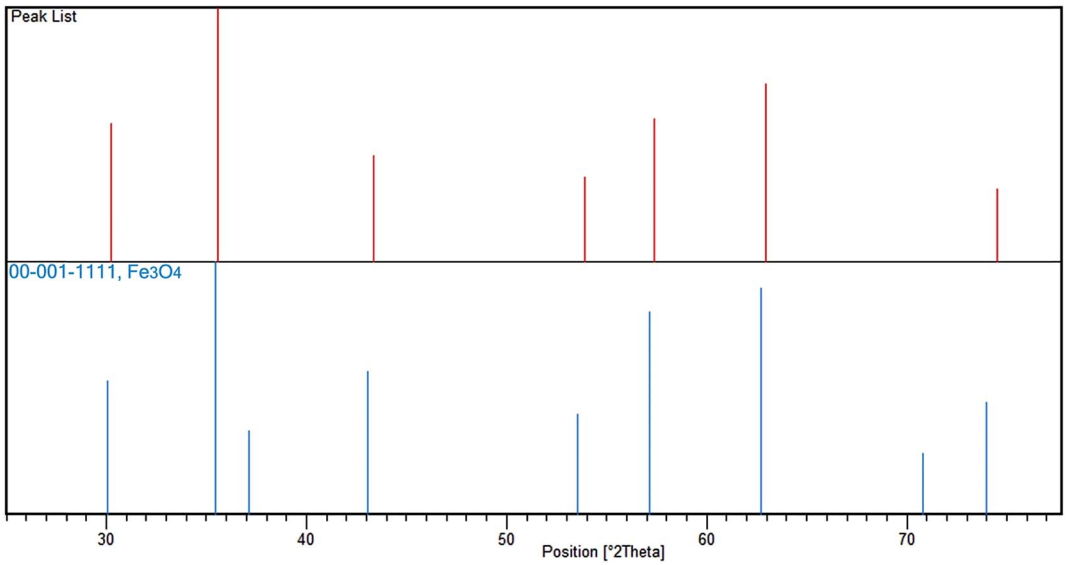

Fig. 3 Pattern of Fe_3O_4@APTES·MAH NPs and standard pattern of magnetite.

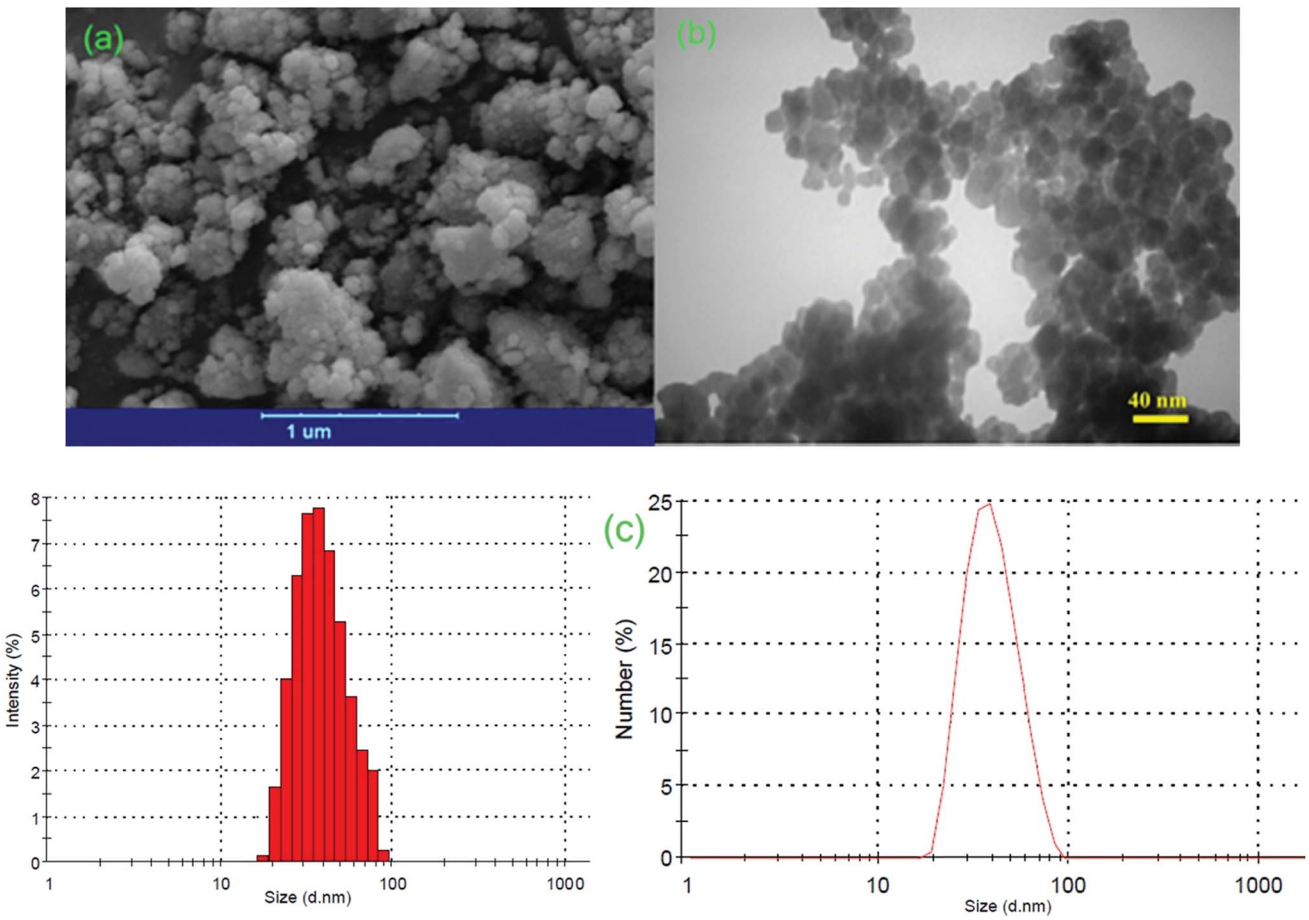

Fig. 4 SEM micrograph (a), TEM image (b) and DLS diagram of Fe_3O_4@APTES·MAH (c).

around 38 nm. Polydispersity index (PDI) for this sample is 0.37 which is an indication of size polydispersity of synthesized Fe_3O_4@APTES·MAH nanospheres.

For stability investigation of the materials, thermogravimetric analysis was used. Fig. 5a–c shows the typical TGA curve of Fe_3O_4 and two modified compounds of it. The organic

materials of the samples are completely burned to generate gas products at the elevated temperature. The weight loss of around 5% below 150 °C for the samples (Fig. 5a and b) is apparently owing to loss of adsorbed water or the water that formed from the condensation of hydroxyl groups. The weight loss between 150 and 600 °C in Fig. 5c was assigned to the breaking of covalent amide bonds and decomposition of acidic catalyst (about 24%). At higher temperature, Fe_3O_4-amine decomposed and iron oxide is formed. Thus, the TGA curve confirmed the successful functionalization of magnetic nanoparticles Fe_3O_4@APTES with maleic anhydride.

The magnetization curves of the magnetic nanoparticles compounds were measured at room temperature with a vibrating sample magnetometry (VSM). As shown in Fig. 6, the saturation magnetizations for Fe_3O_4@APTES (Fig. 6a) and Fe_3O_4@APTES·MAH (Fig. 6b) were found to be 53.01 emu g^{-1} and 39.76 emu g^{-1}, respectively. The saturation magnetization decreased during the function modification process, indicating the reaction of maleic anhydride with amino group and probably with reducing of amino affects the magnetic ability. Fig. 6c and d shows the dispersion of Fe_3O_4@APTES·MAH in ethanol and its separation process, respectively. In the absence of an external magnetic field, the dispersion of Fe_3O_4@APTES·MAH was homogeneous and stable in ethanol. However, this compound was collected easily by applying an external magnetic field. It is very important that a magnetic compound should possess sufficient magnetic properties for easy separation.

Also energy dispersive X-ray spectroscopy (EDAX) results show in Fig. 7 and Table 1 for Fe_3O_4@APTES (a) and Fe_3O_4@APTES·MAH (b). The presence of iron and oxygen can be seen in samples, with iron abundance more than oxygen. Also maleic anhydride adsorption on the surface of Fe_3O_4–APTES nanoparticles is confirmed by the increase in carbon atomic and weight percents.

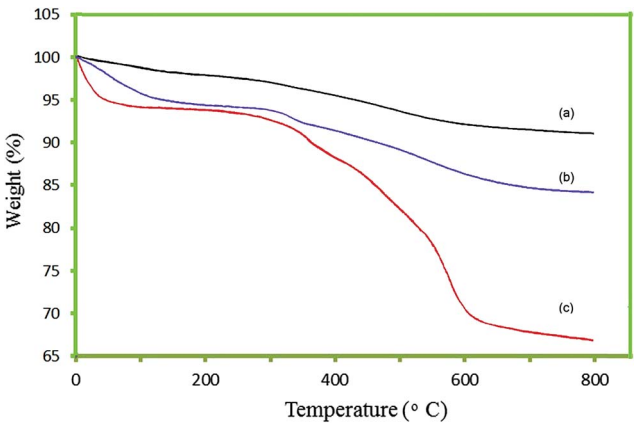

Fig. 5 Thermal gravimetric analysis curves of Fe_3O_4 (a), Fe_3O_4@APTES (b) and Fe_3O_4@APTES·MAH (c).

Catalytic synthesis of bulky heterocyclic compounds

The dialdehydes **1** and **2** were synthesized using the Vilsmeyer reaction according to the literature (Scheme 3).[80,81] 1-Bromobutane or 1-bromohexane was reacted with diphenylamine in the presence of sodium hydroxide in DMSO to give *N*-butyl-*N*-phenylaniline or *N*-hexyl-*N*-phenylaniline, respectively. Under nitrogen atmosphere, $POCl_3$ was added to DMF, then the amine was added to this solution, and the resulting mixture was stirred. After cooling and basified with sodium hydroxide solution, the resulting mixture was extracted and purified by column chromatography to give 4,4′-(hexylazanediyl)dibenzaldehyde (**1**) and 4,4′-(butylazanediyl)dibenzaldehyde (**2**).

Table 2 shows the results of the synthesis of (1,8-dioxodecahydroacridine), bis(1,8-dioxooctahydroxanthene), bis(1,4-dihydropydidine), bis(2,4,5-triarylimidazole), bis(2-cyano-*N*-phenylacrylamide) and bis(dihydropyridine-3,5-dicarbonitrile) derivatives in the presence of modified magnetic nanoparticles. As shown, compounds **3–8** were synthesized in ethanol–water as solvent and, compounds **9–11** under solvent-free conditions at low temperature with good efficiency. The synthesis of compounds **12** and **13** needs a basic catalyst,

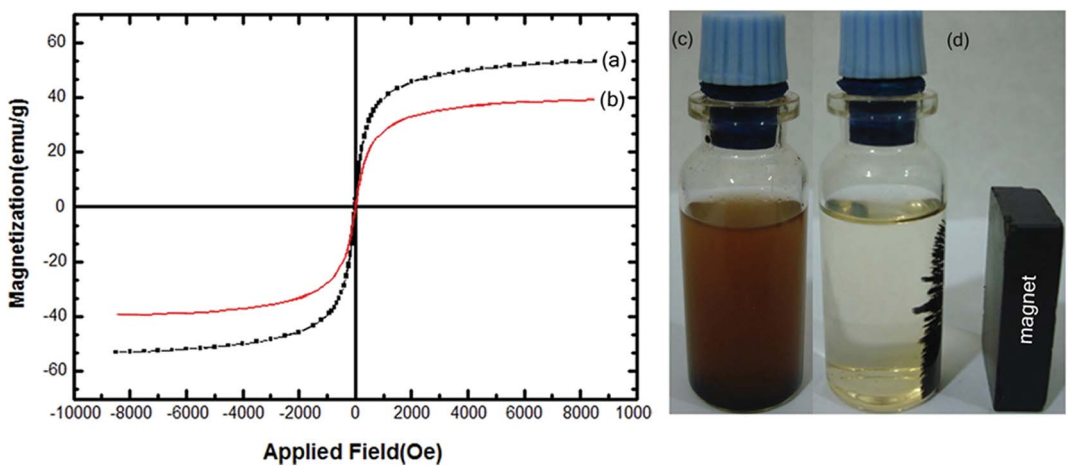

Fig. 6 Magnetization curves at 300 K for Fe_3O_4@APTES NPs (a), Fe_3O_4@APTES·MAH NPs (b), dispersion and separation of Fe_3O_4@APTES·MAH in ethanol without external magnetic field (c), and with external magnetic field (d).

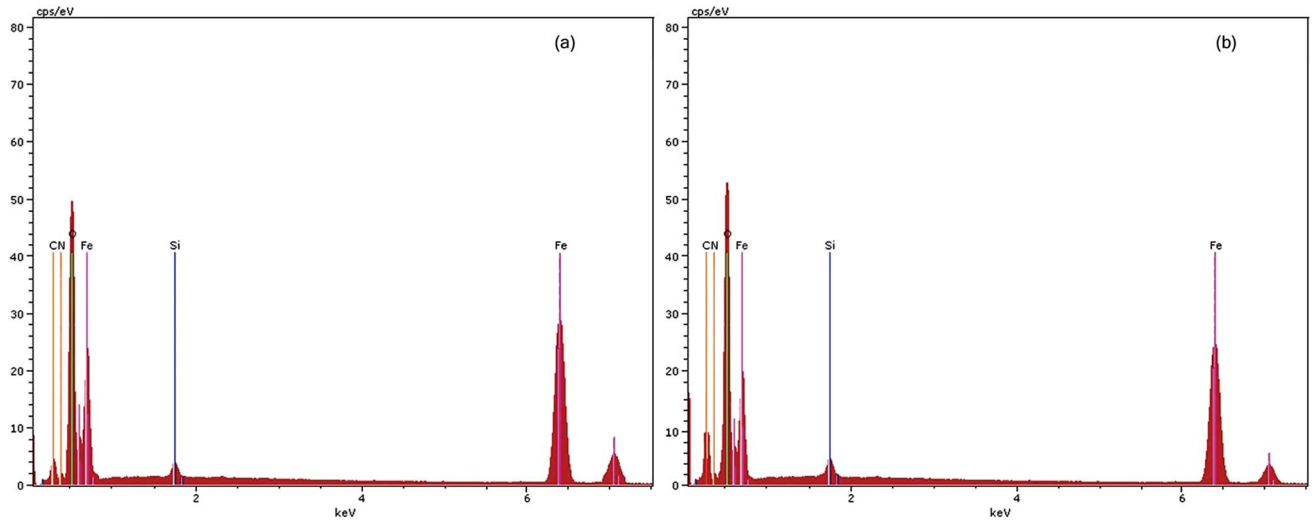

Fig. 7 EDAX results of Fe_3O_4@APTES (a) and Fe_3O_4@APTES·MAH nanoparticles (b).

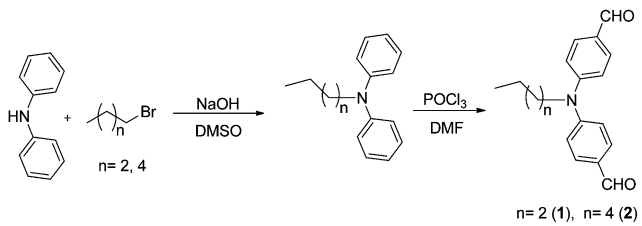

Scheme 3 Synthesis of 4,4′-(alkylazanediyl)dibenzaldehyde.

therefore, triethylamine as a homogeneous catalyst and Fe_3O_4@APTES as a heterogeneous catalyst were used for this purpose (Scheme 4).

Although these compounds in the presence of triethylamine were synthesized with high efficiency, Fe_3O_4@APTES is heterogeneous in the reaction mixture and separate easy by simple magnet. The compound **13** was synthesized using two methods (one-pot, method A and two-step, method B) that first method was more efficient than second procedure (Table 2, entry 11).

For a comparable study on the catalyst effects in reaction efficiencies, synthesis of compounds **3–11** were carried out in the presence of Fe_3O_4@APTES as catalyst (Table 3). It was observed that the reactions using Fe_3O_4@APTES·MAH give excellent yields of products with lower reaction times as compared with the reactions applying Fe_3O_4@APTES that shows low yields. These observations confirm that coating of Fe_3O_4 by APTS does not lead to an acidic catalyst that is necessary for the titled reactions. Therefore, it is obvious that supported MAH moiety induce required acidic character on the catalyst surface leading to efficient progress of the design reactions as shown in Table 3.

It is noteworthy that the catalyst was simply recovered by magnet without any acidic or basic workup even after its five uses. After completion of the reaction of 4,4′-(hexylazanediyl) dibenzaldehyde **2**, ammonium acetate and Fe_3O_4@APTES·MAH for the synthesis of compound **9** at 70 °C, the catalyst was

Table 2 Synthesis of compounds **3–13** catalyzed by modified magnetic nanoparticles

Entry	Comp.	Solvent	Catalyst (g)	Time (min)	Yield (%)	Mp (°C)
1	**3**	Ethanol–water	Fe_3O_4@APTES·MAH (0.08)	130	78	86–88
2	**4**	Ethanol–water	Fe_3O_4@APTES·MAH (0.08)	145	68	140–142
3	**5**	Ethanol–water	Fe_3O_4@APTES·MAH (0.06)	55	80	231–233
4	**6**	Ethanol–water	Fe_3O_4@APTES·MAH (0.06)	48	77	169–171
5	**7**	Ethanol–water	Fe_3O_4@APTES·MAH (0.03)	40	68	161–163
6	**8**	Ethanol–water	Fe_3O_4@APTES·MAH (0.03)	45	70	106–109
7	**9**	Solvent-free	Fe_3O_4@APTES·MAH (0.05)	40	86	92–94
8	**10**	Solvent-free	Fe_3O_4@APTES·MAH (0.08)	35	82	225–227
9	**11**	Solvent-free	Fe_3O_4@APTES·MAH (0.04)	45	69	72–74
10	**12**	1,4-Dioxane	Triethylamine (0.2 mL)	4 (h)	88	140–142
			Fe_3O_4@APTES (0.1)	5 (h)	75	
11	**13** method A	Methanol	Triethylamine (0.2 mL)	5 (h)	72	154–157
			Fe_3O_4@APTES (0.1)	8 (h)	55	
	13 method B	1,4-Dioxane	Triethylamine (0.2 mL)	5 (h)	65	
			Fe_3O_4@APTES (0.1)	8 (h)	50	

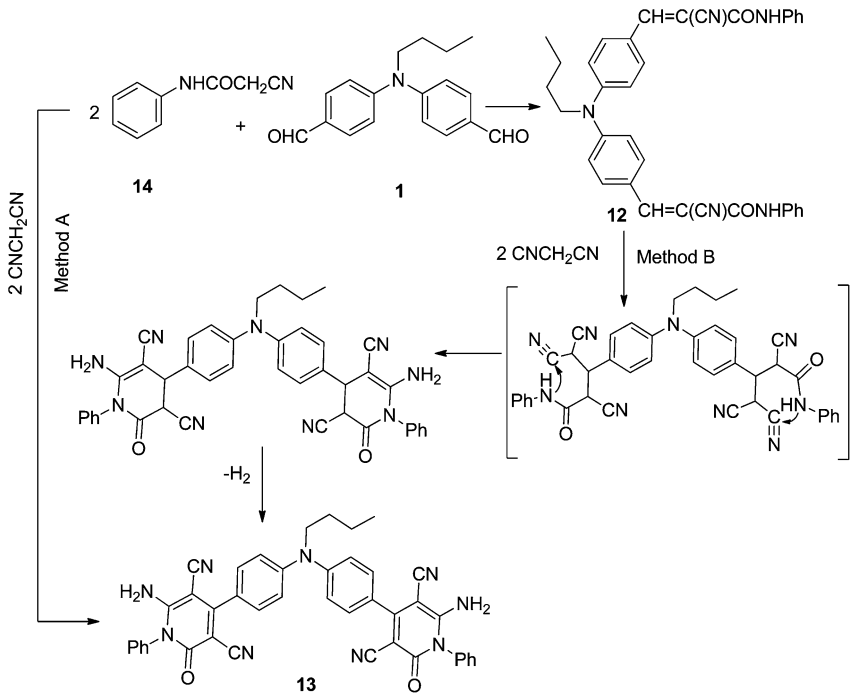

Scheme 4 Synthesis of compound **13** by multicomponent reaction.

Table 3 Efficiency comparison of Fe_3O_4@APTES·MAH as a new catalyst and Fe_3O_4@APTES

			Catalyst (g)/time (min)/yield (%)		
Entry	Comp.	Solvent	Fe_3O_4@APTES·MAH	Fe_3O_4@APTES	Mp (°C)
1	**3**	Ethanol–water	0.08/130/78	0.1/130/12	86–88
2	**4**	Ethanol–water	0.08/145/68	0.1/145/10	140–142
3	**5**	Ethanol–water	0.06/55/80	0.1/55/15	231–233
4	**6**	Ethanol–water	0.06/48/77	0.1/48/15	169–171
5	**7**	Ethanol–water	0.03/40/68	0.1/40/12	161–163
6	**8**	Ethanol–water	0.03/45/70	0.1/45/10	106–109
7	**9**	Solvent-free	0.05/40/86	0.1/40/16	92–94
8	**10**	Solvent-free	0.08/35/82	0.1/35/16	225–227
9	**11**	Solvent-free	0.04/45/69	0.1/45/15	72–74

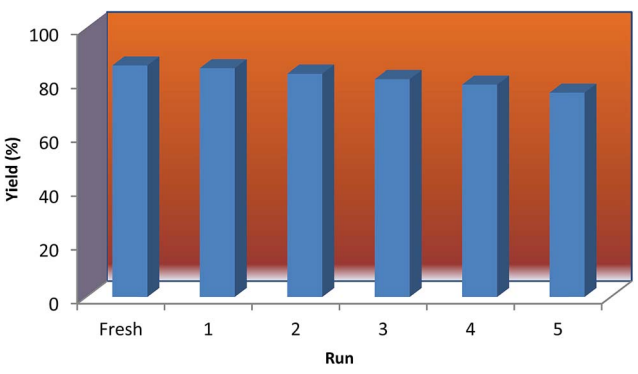

Fig. 8 Recyclability of Fe_3O_4@APTES·MAH in the synthesis of bis(1,4-dihydropyridine) (**9**).

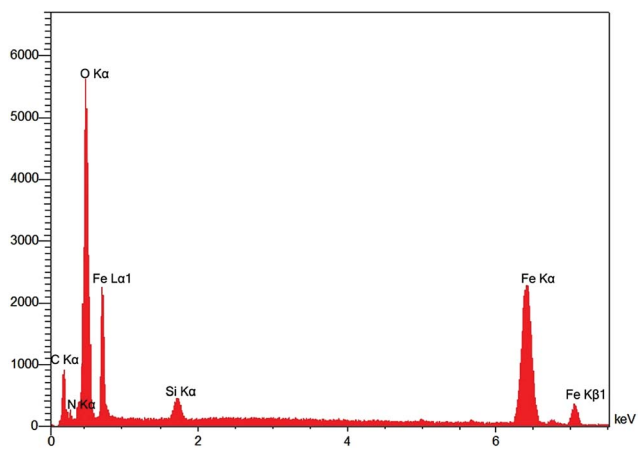

Fig. 9 EDAX results of reused Fe_3O_4@APTES·MAH nanoparticles.

Table 4 Reused catalyst EDAX quantification element normalized

		Fe_3O_4@APTES·MAH reused	
Element	Series	Wt%	At%
Carbon	K-series	12.01	23.73
Nitrogen	K-series	1.41	2.40
Oxygen	K-series	34.47	51.03
Silicon	K-series	1.88	1.59
Iron	K-series	50.23	21.25

recovered from the reaction mixture and recovered catalyst was washed with chloroform and dried. The recovered catalyst was added to fresh substrates under the same experimental conditions for five runs without a significant decrease in the product yield and its catalytic activity (Fig. 8).

The EDAX elemental microanalysis results for the reused Fe_3O_4@APTES·MAH in the synthesis of bis(1,4-dihydropyridine) (**9**) is presented in Fig. 9 and Table 4. Both the fresh catalyst (Fig. 7b) and that recovered after use exhibited similar EDAX patterns (Fig. 9), indicating that the structural properties of the catalyst were not affected by the reaction medium.

Infrared and UV diffusion/reflectance spectra of catalyst before and after reaction are exhibited at Fig. 10 and 11, respectively. The IR peaks appeared at catalyst spectrum after reaction are well in agreement with those obtained for fresh catalyst that confirmed the structure of the catalyst remained unchanged after recycling (Fig. 10). Moreover UV diffusion/reflectance spectrum of fresh catalyst shows five absorption bands in the range of 200–600 nm at 224, 249, 277, 310 and 353 nm wavelengths. As found in Fig. 11b, the used catalyst spectrum also show those electronic transition bands suggesting no notable change in catalyst molecular structure.

Fig. 12 shows DLS of catalyst after the first recovery. In compare between Fig. 4c and 12 can be seen that the catalyst particles have not changed and agglomeration not occurred during the reaction.

In order to show the ability of our method with respect to previous reports, some of our results in comparison to some

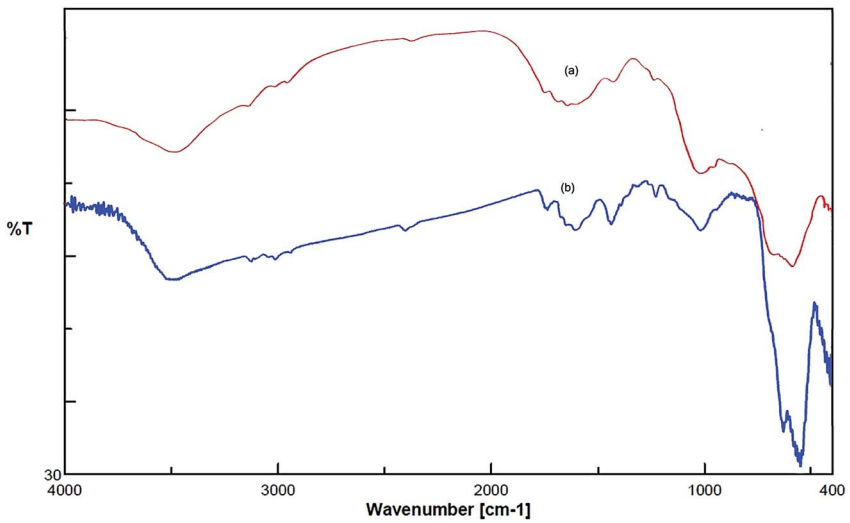

Fig. 10 FT-IR spectra of (a) reused catalyst (b) fresh catalyst.

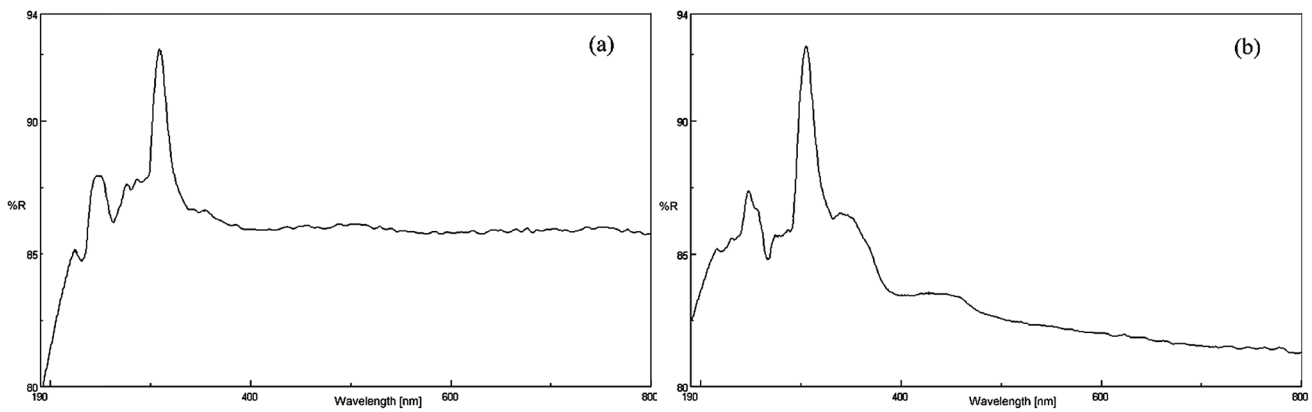

Fig. 11 UV diffusion/reflectance spectrum of (a) fresh catalyst; (b) reused catalyst.

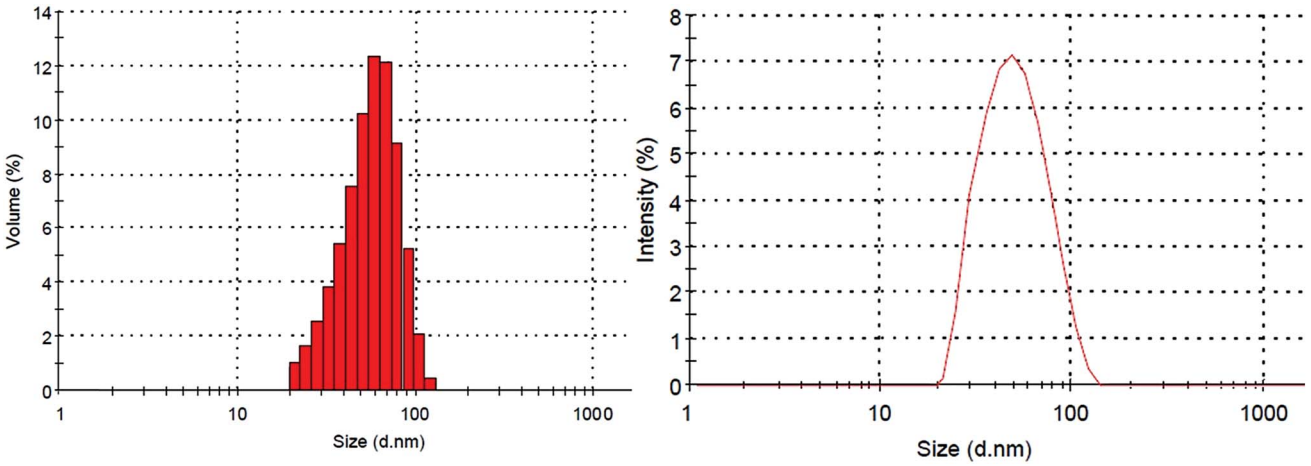

Fig. 12 DLS of reused catalyst.

Table 5 Comparison of efficiency of various catalysts in the synthesis of 1,4-dihydropyrdine, 1,8-dioxooctahydroxanthene, 1,8-dioxo-decahydroacridine, 2-pyridone and imidazole model compounds

Entry	Compound	Catalyst	Conditions	Time (min)	Yield (%)	Ref.
1	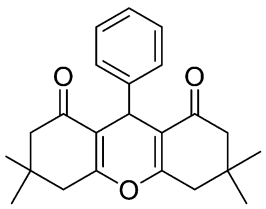	Cellulose sulfonic acid	Solvent-free, 110 °C	300	94	82
		DABCO-bromine	H_2O, reflux	60	90	83
		Fe_3O_4 NPs	Solvent-free, 100 °C	30	86	7
		Fe_3O_4@APTES·MAH	Solvent-free, 70 °C	30	90	—
2	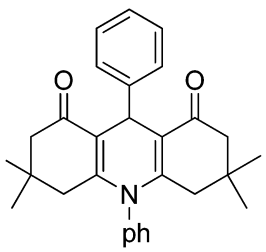	Amberlyst-15	EtOH/reflux	300	81	84
		FSG $Hf(NPf_2)_4$	C_2H_5OH/H_2O, reflux	360	49	85
		Fe_3O_4 NPs	Solvent-free, 120 °C	25	85	8
		Fe_3O_4@APTES·MAH	Solvent-free, 70 °C	35	92	—
3	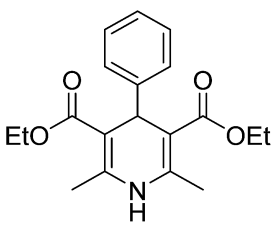	NO	Ultrasonic	40	87	86
		Alumina sulfuric acid	CH_3OH, 70 °C	300	87	87
		Fe_3O_4 NPs	Solvent-free, 80 °C	5	92	5
		Fe_3O_4@APTES·MAH	Solvent-free, 70 °C	10	93	—
4	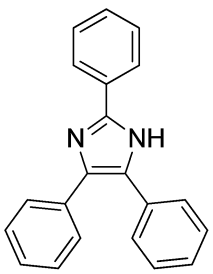	BO_3H_3	C_2H_5OH/H_2O ultrasonic	55	94	88
		Ceric ammonium nitrate	C_2H_5OH/H_2O 65 °C	70	87	89
		Fe_3O_4 NPs	Solvent-free, 80 °C	30	88	9
		Fe_3O_4@APTES·MAH	Solvent-free, 70 °C	30	90	—

Table 6 Catalytic activity of Fe_3O_4@APTES·MAH in various organic reactions compared with Fe_3O_4 NPs

		Fe_3O_4@APTES·MAH			Fe_3O_4 NPs			
Entry	Product	Condition	Time	Yield (%)	Condition	Time	Yield (%)	Ref.
1	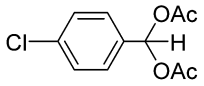	Solvent-free 50 °C	30 (min)	86	Solvent-free 50 °C	30 (min)	48	—
2	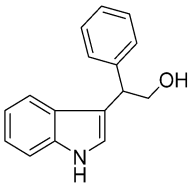	CH_3CN 50 °C	10 (h)	67	Neat RT[a]	24 (h)	65	90
3	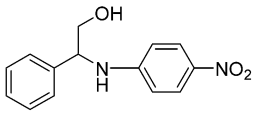	CH_3CN 60 °C	8 (h)	70	Neat RT[a]	20 (h)	65	91
4	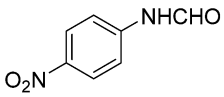	CH_3CN reflux	80 (min)	90	PEG_{400}70 °C[a]	90 (min)	85	92

[a] The amount of catalyst: 0.023 g.

other methods are summarized in Table 5. To compare between the effect of magnetic nanoparticles (Fe_3O_4 NPs), modified magnetic nanoparticles (Fe_3O_4@APTES·MAH) and other catalysts, benzaldehyde was used as a model substrate. As shown in Table 3 by using Fe_3O_4@APTES·MAH, the reaction carried out in a moderate temperature with high efficiency and the yield/time ratio of the present method is better or comparable with the other reported results.

Furthermore, to show the catalytic activity of the Fe_3O_4@APTES·MAH as compared with Fe_3O_4 NPs in other cases, some organic reactions such as acylal synthesis (entry 1), epoxide reaction with indole (entry 2), aminolysis of epoxide (entry 3) and *N*-formylation of amine (entry 4) in Table 6, were selected and run in the presence of Fe_3O_4@APTES·MAH (Scheme 5) and then the results were compared with those reported using Fe_3O_4 NPs in the literature. As shown in Table 6, in all designed reactions, the catalyst of Fe_3O_4@APTES·MAH (as Brønsted acid) catalyzed the reactions with more ratios of yield/time with respect to Fe_3O_4 (as Lewis acid). With regard to the above comparative reactions, it seems that the Fe_3O_4@APTES·MAH can be recommended as a new Brønsted acid for many organic reactions that need the acid catalyst.

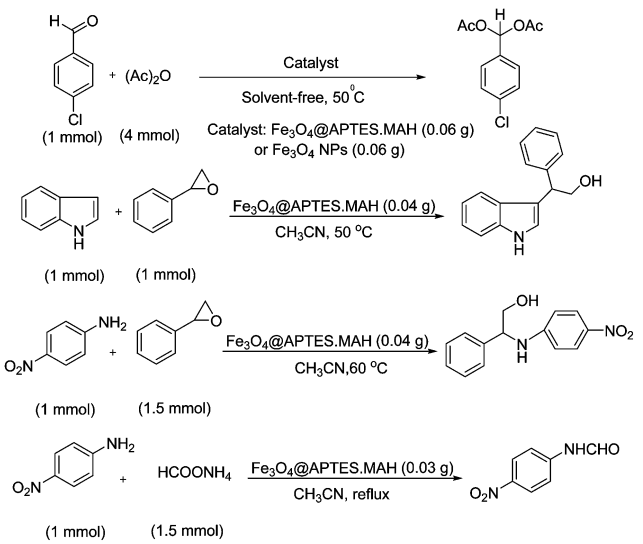

Scheme 5 Different comparative reactions.

Conclusions

Fe_3O_4 NPs are an efficient acidic catalyst for synthesis of numerous heterocyclic compounds. When Fe_3O_4 was coated with γ-aminopropyltriethyoxysilane (Fe_3O_4–APTES) not only reduced acidic properties but also used as a base catalyst. This assertion is proved for synthesis of compounds **12** and **13** (Method A) in the presence of this catalyst. Although the effect of this catalyst is lower than triethylamine (longer times and lower yields). In summary, we showed that maleic anhydride reacted with NH_2 coated Fe_3O_4 nanoparticles and produced acidic catalyst that was a novel and effective heterogeneous and magnetic catalyst for the one-pot synthesis of heterocyclic compounds. The present method requires remarkably small amounts of non-toxic and environmentally friendly Fe_3O_4–APTES·MAH as a catalyst. In addition we introduced magnetically nanocatalyst that could be reused in 5 successive runs with no significant structural change and loss of activity.

Acknowledgements

We are grateful to the Yasouj University for financial assistance.

References

1 B. V. Subba Reddy, A. Siva Krishna, A. V. Ganesh and G. G. K. S. Narayana Kumar, *Tetrahedron Lett.*, 2011, **52**, 1359–1362.
2 Z. H. Zhang, H. Y. Lu, S. H. Yang and J. W. Gao, *J. Comb. Chem.*, 2010, **12**, 643–646.
3 M. Nasr-Esfahani, S. J. Hoseini and F. Mohammadi, *Chin. J. Catal.*, 2011, **32**, 1484–1489.
4 R. Cano, D. J. Ramon and M. Yus, *Synlett*, 2001, 2017–2019.
5 M. Nasr-Esfahani, S. J. Hoseini, M. Montazerozohori, R. Mehrabi and H. Nasrabadi, *J. Mol. Catal. A: Chem.*, 2014, **382**, 99–105.
6 B. Karami, S. J. Hoseini, S. Nikoseresht and S. Khodabakhshi, *Chin. Chem. Lett.*, 2012, **23**, 173–176.
7 M. A. Ghasemzadeh, J. Safaei-Ghomi and S. Zahedi, *J. Serb. Chem. Soc.*, 2013, **78**, 769–779.
8 M. A. Ghasemzadeh, J. Safaei-Ghomi and H. Molaei, *C. R. Chim.*, 2012, **15**, 969–974.
9 B. Karami, K. Eskandari and A. Ghasemi, *Turk. J. Chem.*, 2012, **36**, 601–614.
10 R. Martinez, D. J. Ramon and M. Yus, *Adv. Synth. Catal.*, 2008, **350**, 1235–1240.
11 M. M. Mojtahedi, M. S. Abaee and T. Alishiri, *Tetrahedron Lett.*, 2009, **50**, 2322–2325.
12 H. Yang, Y. Zhuang, Y. Sun, A. Dai, X. Shi, D. Wu, F. Li, H. Hu and S. Yang, *Biomaterials*, 2011, **32**, 4584–4593.
13 J. M. Petez, F. J. Simeone, Y. Saski, L. Josephson and R. Weissleder, *J. Am. Chem. Soc.*, 2003, **125**, 10192–10193.
14 M. W. Shen and X. Shi, *Nanoscale*, 2010, **2**, 1596–1610.
15 Y. Ling, K. Wei, Y. Luo, X. Gao and S. Zhong, *Biomaterials*, 2011, **32**, 7139–7150.
16 S. Purushotham and R. V. Ramanujan, *Acta Biomater.*, 2010, **6**, 502–510.
17 Z. Q. Samra, S. Shabir, Z. Rehmat, M. Zaman, A. Nazir, N. Dar and M. A. Athar, *Appl. Biochem. Biotechnol.*, 2010, **162**, 671–678.
18 M. H. Mashhadizadeh, M. Amoli-Diva, M. R. Shapouri and H. Afruzi, *Food Chem.*, 2014, **151**, 300–305.
19 W. C. Song, M. C. Liu, R. Hu, X. L. Tan and J. X. Li, *Chem. Eng. J.*, 2014, **246**, 268–276.
20 J. K. Xu, F. F. Zhang, J. J. Sun, J. Sheng, F. Wang and M. Sun, *Molecules*, 2014, **19**, 21506–21528.
21 R. G. Chaudhuri and S. Paria, *Chem. Rev.*, 2012, **112**, 2373–2433.
22 R. Tadmor, R. E. Rosensweig, J. Frey and J. Klein, *Langmuir*, 2000, **16**, 9117–9120.
23 A. K. Gupta and M. Gupta, *Biomaterials*, 2005, **26**, 3995–4021.
24 M. H. Sousa, J. C. Rubim, P. G. Sobrinho and F. A. Tourinho, *J. Magn. Magn. Mater.*, 2001, **225**, 67–72.
25 P. C. Morais, A. C. Oliveira, A. L. Tronconi, T. Goetze and N. Buske, *IEEE Trans. Magn.*, 2003, **39**, 2654–2656.
26 X. C. Shen, X. Z. Fang, Y. H. Zhou and H. Liang, *Chem. Lett.*, 2004, **33**, 1468–1469.
27 X. Liu, Z. Ma, J. Xing and H. Liu, *J. Magn. Magn. Mater.*, 2004, **270**, 1–6.
28 Z. Yinghuai, S. C. Peng, A. Emi, S. Zhenshun, M. Lisa and R. A. Kemp, *Adv. Synth. Catal.*, 2007, **349**, 1917–1922.
29 R. Abu-Reziq, H. Alper, D. Wang and M. L. Post, *J. Am. Chem. Soc.*, 2006, **128**, 5279–5282.
30 S. Luo, X. Zheng, H. Xu, X. Mi, L. Zhang and J. P. Cheng, *Adv. Synth. Catal.*, 2007, **349**, 2431–2434.
31 M. Kawamura and K. Sato, *Chem. Commun.*, 2007, 3404–3405.
32 M. Hatamzadeh, M. Johari-Ahar and M. Jaymand, *Int. J. Biomed. Nanosci. Nanotechnol.*, 2012, **8**, 51–60.
33 F. Hosseini, M. Seyedsajadi and N. Farhadyar, *O. J. Chem.*, 2014, **30**, 1609–1618.
34 B. Feng, R. Y. Hong, L. S. Wang, L. Guo, H. Z. Li, J. Ding, Y. Zheng and D. G. We, *Colloids Surf., A*, 2008, **328**, 52–59.
35 T. Poursaberi, H. Ghanbarnejad and V. Akbar, *J. Neurosurg.*, 2013, **2**, 417–426.
36 M. Shen, H. Cai, X. Wang, X. Cao, K. Li, S. H. Wang, R. Guo, L. Zheng, G. Zhang and X. Shi, *Nanotechnology*, 2012, **23**, 105601, DOI: 10.1088/0957-4484/23/10/105601.
37 J. Safari and Z. Zarnegar, *Ultrason. Sonochem.*, 2013, **20**, 740–746.
38 A. R. Karimi, M. Sourinia, Z. Dalirnasab and M. Karimi, *Can. J. Chem.*, 2015, **93**, 546–549.
39 M. M. A. Nikje, L. Sarchami and L. Rahmani, *Int. J. Biomed. Nanosci. Nanotechnol.*, 2015, **11**, 39–44.
40 R. A. Reziq and H. Alper, *Appl. Sci.*, 2012, **2**, 260–276.
41 P. B. Bhat and B. R. Bhat, *New J. Chem.*, 2015, **39**, 273–278.
42 A. Krauze, S. Germane, O. Eberlins, I. Sturms, V. Klusa and G. Duburs, *Eur. J. Med. Chem.*, 1999, **34**, 301–310.
43 T. Tsuruo, H. Iida, M. Nojiri, S. Tsukagoshi and Y. Sakurai, *Cancer Res.*, 1983, **43**, 2905–2910.
44 W. J. Malaise and P. C. F. Mathias, *Diabetologia*, 1985, **28**, 153–156.
45 X. Zhou, L. Zhang, E. Tseng, E. Scott-Ramsay, J. J. Schentag, R. A. Coburn and M. E. Morris, *Drug Metab. Dispos.*, 2005, **33**, 321–328.
46 K. Aouam and A. Berdeaux, *Therapie*, 2003, **58**, 333–339.
47 A. R. Trivedi, D. K. Dodiya, B. H. Dholariya, V. B. Kataria, V. R. Bhuva and V. H. Shah, *Bioorg. Med. Chem. Lett.*, 2011, **21**, 5181–5183.
48 M. Khoshneviszadeh, N. Edraki, K. Javidnia, A. Alborzi, B. Pourabbas, J. Mardaneh and R. Mir, *Bioorg. Med. Chem.*, 2009, **17**, 1579–1586.
49 R. W. Lambert, J. A. Martin, J. H. Merrett, K. E. B. Parkes and G. J. Thomas, PCT Int. Appl., WO 9706178, 1997trans*Chem. Abstr.*, 1997, 126, 212377y.
50 T. Hideo, *Chem. Abstr.*, 1981, 95, 80922btransJpn. Tokyo Koho JP 56005480, 1981.
51 R. M. Ion, D. frackowiak, A. Planner and K. Wiktorowicz, *Acta Biochim. Pol.*, 1998, **45**, 833–845.
52 S. Harkishan and V. K. Kapoor, *Medicinal and Pharmaceutical Chemistry*, Vallabh Prakashan, Delhi, 2nd edn, 2005, pp. 364–365 and 473-475.
53 M. A. Horstmann, W. A. Hassenpflug, U. zur Stadt, G. Escherich, G. Janka and H. Kabisch, *Haematologica*, 2005, **90**, 1701–1703.

54 A. Islam, P. Murugan, K. C. Hwang and C. H. Cheng, *Synth. Met.*, 2003, **139**, 347–354.
55 S. J. Tu, C. Miao, Y. Gao, F. Fang, Q. Zhuang, Y. Feng and D. Shi, *Synlett*, 2004, **2**, 255–258.
56 N. S. Burres, S. Sazesh, G. P. Gunawardana and J. J. Clement, *Cancer Res.*, 1998, **49**, 5267–5274.
57 D. Greenwood, *J. Antimicrob. Chemother.*, 1995, **36**, 857–872.
58 M. Wainwright, *J. Antimicrob. Chemother.*, 2001, **47**, 1–13.
59 O. Berkan, B. Sarac, R. Simsek, S. Yildirim, Y. Sariogli and C. Safak, *Eur. J. Med. Chem.*, 2002, **37**, 519–523.
60 (*a*) U. Holzgrabe, *Pharm. Unserer Zeit*, 2001, **30**, 446–448; (*b*) Q. Li, L. A. Mitscher and L. L. Shen, *Med. Res. Rev.*, 2000, **20**, 231–293.
61 A. K. Gupta and T. Plott, *Int. J. Dermatol.*, 2004, **43**, 3–8.
62 J. L. Medina-Franco, K. Martínez-Mayorga, C. Juárez-Gordiano and R. Castillo, *ChemMedChem*, 2007, **2**, 1141–1147.
63 S. Brickner, *Chem. Ind.*, 1997, 131–135.
64 I. Collins, C. Moyes, W. B. Davey, M. Rowley, F. A. Bromidge, K. Quirk, J. R. Atack, R. M. McKernan, S. A. Thompson, K. Wafford, G. R. Dawson, A. Pike, B. Sohal, N. N. Tsou, R. G. Bull and J. L. Castro, *J. Med. Chem.*, 2002, **45**, 1887–1900.
65 (*a*) M. Endoh and M. Hori, *Expert Opin. Pharmacother.*, 2006, **7**, 2179–2202; (*b*) N. Robert, C. Verrier, C. Hoarau, S. Celanire and F. Marsais, *ARKIVOC*, 2008, **7**, 92–100.
66 U. Domanska and M. K. Kozlowska, *Fluid Phase Equilib.*, 2003, **206**, 253–266.
67 A. K. Tackle, M. J. B. Brown, S. Davies, D. K. Dean, G. Francis, A. Gaiba, A. W. Hird, F. D. King, P. J. Lovell, A. Naylor, A. D. Reith, J. G. Steadman and D. M. Wilson, *Bioorg. Med. Chem. Lett.*, 2006, **16**, 378–381.
68 J. C. Lee, J. T. Laydon, P. C. McDonnell, T. F. Gallagher, S. Kumar, D. Green, D. McNulty, M. J. Blumenthal, J. R. Keys, S. W. L. Vatter, J. E. Strickler, M. M. McLughlin, I. R. Siemens, S. M. Fisher, G. P. Livi, J. R. White, J. L. Adams and P. R. Young, *Nature*, 1994, **372**, 739–746.
69 L. Wang, K. W. Woods, Q. Li, K. J. Barr, R. W. McCroskey, S. M. Hannick, L. Gkerke, R. B. Credo, Y. H. Hui, K. Marsh, R. Warener, J. Y. Lee, N. Zielinsky-Mozng, D. Frost, S. H. Rosenberg and H. L. Sham, *J. Med. Chem.*, 2002, **45**, 1697–1711.
70 S. E. De Laszlo, C. Hacker, B. Li, D. Kim, M. MacCoss, N. Mantlo, J. V. Pivnichny, L. Colwell, G. E. Koch, M. A. Cascieri and W. K. Hagmenn, *Bioorg. Med. Chem. Lett.*, 1999, **9**, 641–646.
71 S. Chen, Z. Xu, H. Dai and S. Zhang, *J. Alloys Compd.*, 2010, **497**, 221–227.
72 M. P. Calatayud, B. Sanz, V. Raffa, C. Riggio, M. R. Ibarra and G. F. Goya, *Biomaterials*, 2014, **35**, 6389–6399.
73 M. Esmaeilpour, J. Javidi, F. Nowroozi-Dodeji and M. Mokhtari-Abarghoui, *J. Mol. Catal. A: Chem.*, 2014, **393**, 18–29.
74 R. Massart, *IEEE Trans. Magn.*, 1981, **17**, 1247–1248.
75 W. W. Yu, E. Chang, J. C. Falkner, J. Zhang, A. M. Al-Somali, C. M. Sayes, J. Johns, R. Drezek and V. L. Colvin, *J. Am. Chem. Soc.*, 2007, **129**, 2871–2879.
76 S. J. Hoseini, H. Nasrabadi, M. Azizi, A. Salimi-Beni and R. Khalifeh, *Synth. Commun.*, 2013, **43**, 1683–1691.
77 B. Hu, J. Pan, H. L. Yu, J. W. Liu and J. H. Xu, *Process Biochem.*, 2009, **44**, 1019–1024.
78 T. Phenrat, H. J. Kim, F. Fagerlund, T. Illangasekare, R. D. Tilton and G. V. Lowry, *Environ. Sci. Technol.*, 2009, **43**, 5079–5085.
79 I. Y. Goon, L. M. H. Lai, M. Lim, P. Munroe, J. J. Gooding and R. Amal, *Chem. Mater.*, 2009, **21**, 673–681.
80 D. J. Kim, S. H. Kim, T. Zyung, J. J. Kim, I. Cho and S. K. Choi, *Macromolecules*, 1996, **29**, 3657–3660.
81 S. Ramkumar, S. Manoharan and S. Anandan, *Dyes Pigm.*, 2012, **94**, 503–511.
82 H. A. Oskooie, L. Tahershamsi, M. M. Heravi and B. Baghernejad, *Chem.–Eur. J.*, 2010, **7**, 717–720.
83 M. Bigdeli, *Chin. Chem. Lett.*, 2010, **21**, 1180–1182.
84 B. Das, P. Thirupathi, I. Mahender, V. S. Reddy and Y. K. Rao, *J. Mol. Catal. A: Chem.*, 2006, **247**, 233–239.
85 M. Hong and G. Xiao, *J. Fluorine Chem.*, 2012, **144**, 7–9.
86 S. X. Wang, Z. Y. Li, J. C. Zhang and J. T. Li, *Ultrason. Sonochem.*, 2008, **15**, 677–680.
87 M. Arsalan, C. Faydali, M. Zengin and H. Demirhan, *Turk. J. Chem.*, 2009, **33**, 769–774.
88 K. F. Shelke, S. B. Sapkal, S. S. Sonar, B. R. Madje, B. B. Shingate and M. S. Shingare, *Bull. Korean Chem. Soc.*, 2009, **30**, 1057–1060.
89 J. N. Sangshetti, N. D. Kokare, S. A. Kotharkara and D. B. Shinde, *J. Chem. Sci.*, 2008, **120**, 463–467.
90 R. Parella, Naveen and S. A. Babu, *Catal. Commun.*, 2012, **29**, 118–121.
91 A. Kumar, R. Parella and S. A. Babu, *Synlett*, 2014, **25**, 835–842.
92 Z. G. Wang and M. Lu, *RSC Adv.*, 2014, **4**, 1234–1240.